

2013-05-07

A Scaffold Model of the Outer Retina

Kristina R. Russano

University of Miami, krussano@med.miami.edu

Follow this and additional works at: https://scholarlyrepository.miami.edu/oa_theses

Recommended Citation

Russano, Kristina R., "A Scaffold Model of the Outer Retina" (2013). *Open Access Theses*. 419.
https://scholarlyrepository.miami.edu/oa_theses/419

This Embargoed is brought to you for free and open access by the Electronic Theses and Dissertations at Scholarly Repository. It has been accepted for inclusion in Open Access Theses by an authorized administrator of Scholarly Repository. For more information, please contact repository.library@miami.edu.

UNIVERSITY OF MIAMI

A SCAFFOLD MODEL OF THE OUTER RETINA

By

Kristina R. Russano

A THESIS

Submitted to the Faculty
of the University of Miami
in partial fulfillment of the requirements for
the degree of Master of Science

Coral Gables, Florida

May 2013

©2013
Kristina R. Russano
All Rights Reserved

UNIVERSITY OF MIAMI

A thesis submitted in partial fulfillment of
the requirements for the degree of
Master of Science

A SCAFFOLD MODEL OF THE OUTER RETINA

Kristina R. Russano

Approved:

Ozcan Ozdamar, Ph.D.
Professor of Biomedical Engineering

M. Brian Blake, Ph.D.
Dean of the Graduate School

Herman Cheung, Ph.D.
Professor of Biomedical Engineering

Fotios Andreopoulos, Ph.D.
Associate Professor of Biomedical
Engineering

Jeffrey Goldberg, M.D., Ph.D.
Associate Professor of Ophthalmology

RUSSANO, KRISTINA R.
A Scaffold Model of the Outer Retina

(M.S., Biomedical Engineering)
(May 2013)

Abstract of a thesis at the University of Miami.

Thesis supervised by Professor Jeffrey Goldberg.
No. of pages in text. (36)

Patients with diseases that lead to the loss of the cells of their outer retina, such as AMD and retinitis pigmentosa, suffer from an irreversible loss of vision. Since the body has no mechanism to restore the structure or function of these cells, could photoreceptors be transplanted to restore function? Several groups have attempted transplantations, but were faced with the challenges of low retention and inefficient delivery. Also, a limitation of photoreceptor research is their poor survival in culture due to their dependence on RPE. We propose that a two-layered biodegradable polymer scaffold that serves as support and a permeable barrier between photoreceptors and RPE could provide support and enhance photoreceptor integration at the target site. This type of system will increase the survival of the photoreceptors by nurturing their dependence on RPE. Also, this scaffold will increase the efficiency of cell delivery by increasing the availability of the photoreceptors and therefore their chances of integration at the desired site. An electrospun scaffold was chosen for this application because a permeable scaffold can support cell retention, act as a barrier, while also allowing the two cell types to interact. This novel co-delivery was possible because we electrospun polylactic acid fibers on top of living RPE cells and seeded photoreceptors on top of the fibers. We used scanning electron microscopy, a Live/Dead cell assay, and immunohistochemistry to prove our hypothesis that it is possible to electrospin PLA scaffolds with consistent fiber diameters

on top of living RPE cells, the cells are able to recover and display the same viability as control samples, and the scaffolds provide the support necessary for the seeded photoreceptors to remain separated and above the RPE layer.

Acknowledgements

I would like to gratefully acknowledge the scientific contributions of Dr. Karl Kador and Dr. Enrique Salero. All the RPE cultures used in this work were established by Enrique Salero. Electrospinning, photoreceptor harvesting, and scaffold seeding were done in collaboration with Karl Kador.

Table of Contents

| | |
|--|-----------|
| List of Figures..... | v |
| Chapter 1: A Scaffold Model of the Outer Retina..... | 1 |
| Chapter 2: Methods..... | 14 |
| Isolation and Culturing of Retinal Pigment Epithelium..... | 14 |
| Electrospinning Polylactic Acid on top of Retinal Pigment Epithelium..... | 14 |
| Live/ Dead Assay of Retinal Pigment Epithelium after Electrospinning..... | 16 |
| Scanning Electron Microscopy of RPE/PLA Scaffold..... | 16 |
| Harvesting an Enriched-Photoreceptor Suspension and Seeding..... | 17 |
| Immunohistochemistry..... | 17 |
| Chapter 3: Results..... | 19 |
| Electrospun Polylactic Acid Fiber Size..... | 19 |
| Retinal Pigment Epithelium Survival after Electrospinning..... | 20 |
| Retinal Pigment Epithelium and Photoreceptor Separation..... | 23 |
| Chapter 4: Discussion..... | 29 |
| Chapter 5: Conclusion..... | 32 |
| References..... | 33 |

List of Figures

| | |
|---|----|
| Figure 1 <i>Cell Layers of the Retina</i> | 2 |
| Figure 2 <i>Fluorescence Microscopy of Retinal Layers</i> | 3 |
| Figure 3 <i>Fluorescence Microscopy of the Nerve Fiber Layer</i> | 3 |
| Figure 4 <i>Schematic of Electrospinning Process</i> | 11 |
| Figure 5 <i>Electrospinning Parameter Variations and Resulting Diameters</i> | 19 |
| Figure 6 <i>SEM of Cultured RPE Cells beneath PLA Fibers</i> | 20 |
| Figure 7 <i>Fluorescence Microscopy of RPE Cells beneath PLA Fibers</i> | 21 |
| Figure 8 <i>Confocal Microscopy of RPE with Scaffold Removed</i> | 21 |
| Figure 9 <i>Fluorescence Microscopy of RPE Confluence under Fibers</i> | 22 |
| Figure 10 <i>Live/Dead Assay of RPE after Electrospinning</i> | 23 |
| Figure 11 <i>Velocity Confocal Image above Scaffold</i> | 25 |
| Figure 12 <i>Cross Section through z-axis of Velocity Image of Scaffold</i> | 25 |
| Figure 13 <i>Cross section through z-axis of Velocity Image of control sample</i> | 25 |
| Figure 14 <i>Measurement of Fluorescence Emitted from Photoreceptors and RPE along the z-axis of a Scaffold Sample</i> | 26 |
| Figure 15 <i>Measurement of Fluorescence Emitted from Photoreceptors and RPE along the z-axis of a Control Sample</i> | 26 |
| Figure 16 <i>Quantification of the Separation of Photoreceptors and RPE along the z-axis of Scaffold and Control Samples</i> | 27 |
| Figure 17 <i>Photoreceptor Outer Segments Extending Downward on Scaffold (10X)</i> ... | 28 |
| Figure 18 <i>Photoreceptor Outer Segments Extending Downward on Scaffold (40X)</i> ... | 28 |

Chapter 1: A Scaffold Model of the Outer Retina

When light enters the eye, it is transmitted through the cornea and lens onto the retina in the back of the eye. The retina consists of distinct layers of different cell types and has a highly structured three dimensional architecture. It is also responsible for transducing light into electrical signals that travel to the brain for the perception of images. When light enters the eye, it must travel through the ganglion, inner, and outer nuclear layers to reach the outer segments of the photoreceptors, where a reaction begins in response to the light. The electrical signal produced from this reaction travels in the opposite direction of the light path. It travels from the photoreceptors to the ganglion cells, which create an action potential that projects down their axons (Bear, Connors et al. 2001). The axons of ganglion cells bundle together to form the nerve fiber layer and project radially towards the back of the eye to form the optic nerve (Figure 1). Finally, the optic nerve carries the signal to the targets in the brain.

The outer nuclear layer of the retina contains the cells bodies of the photoreceptors, while their outer segments are restricted within their own layer. The outer segments of these cells are structured with stacks of discs that contain light-reactive photopigments. The cell bodies of the bipolar, amacrine, and horizontal cells reside in the next layer, the inner nuclear. Bipolar cells receive a signal from the photoreceptors and pass it along to the ganglion cells. The bipolar cells synapse with photoreceptors in the outer plexiform layer, while the horizontal cells synapse laterally in the same layer. The inner most layer of the retina is the ganglion cell layer which contains the ganglion cell bodies. These cells are the only cells of the retina that can create an action potential. The ganglion cells synapse with bipolar cells in the inner plexiform layer of the retina. The

synaptic regions of amacrine cells are also in this layer, but they connect laterally to the bipolar and ganglion cells in order to modify their signals.

The light reactive photoreceptors that start the signaling process are dependent on a monolayer of cells, called the retinal pigment epithelium. The retinal pigment epithelium is a monolayer of cells that make up the outer most layer of the retina (Purves, Augustine et al. 2001). RPE cells are involved in the maintenance of the photoreceptor outer segments and their photopigments (Bandyopadhyay and Rohrer 2010). Due to their pigmentation, RPE are also able to absorb any refracted light which could distort the perception of an image.

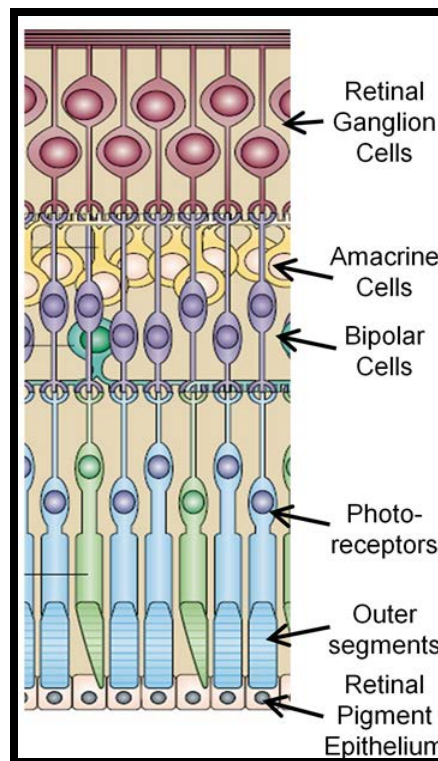


Figure 1 – Cell layers of the Retina (Diagram by JL Goldberg, unpublished)

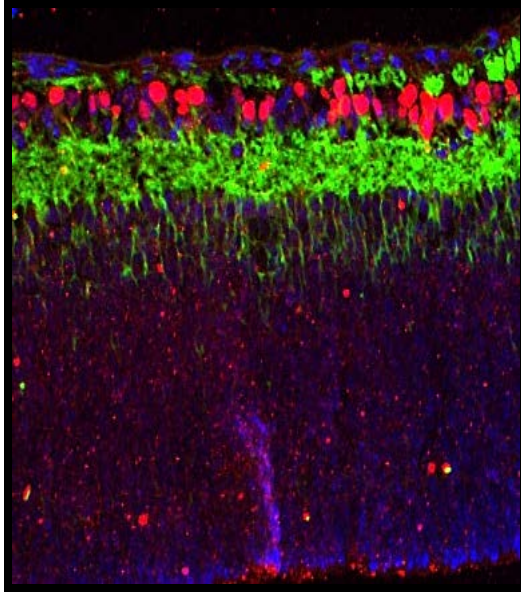


Figure 2 – Fluorescence Microscopy of Retinal Layers. Brn3 staining of RGCs (red) and beta-III tubulin staining of neurites (green). Photoreceptors are located near the bottom of the image. (Diagram by J Hertz, unpublished)

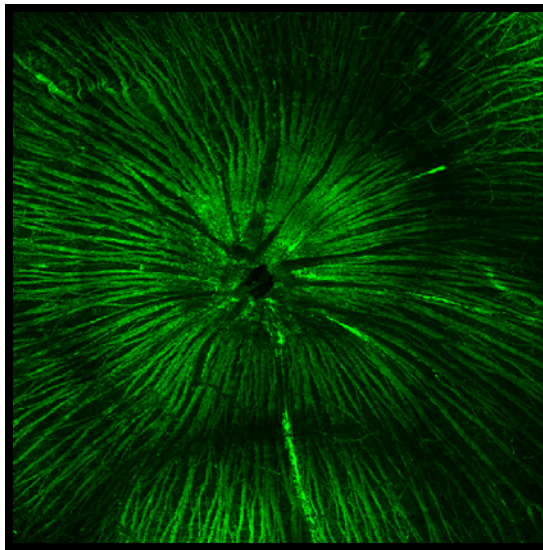


Figure 3 – Fluorescence microscopy of nerve fiber layer of retinal explant with beta III-tubulin immunostaining (Image by K Kador, unpublished)

During development, the optic nerve and retina originate from the brain and are therefore considered part of the central nervous system (Bear, Connors et al. 2001). Like other cells of the central nervous system, photoreceptors fail to regenerate after injury or disease such as age-related macular degeneration (AMD) or retinitis pigmentosa (Margalit and Sadda 2003). Unfortunately, the body does not have a way to restore the structure or function of these cells once they have degenerated. AMD is a leading cause of blindness and visional impairment in adults. Patients with AMD experience a reduction in visual acuity due to damage of the photoreceptors in the macula. In the “dry” form of this disease, cellular debris accumulates behind the retina leading to damage. On the other hand, “wet” AMD, a more severe disease, is caused by blood vessel growth into the retina. Eventual vessel leakage and resulting cellular atrophy can cause retinal detachment and further damage (Roberts 2006). Increased levels of VEGF (vascular endothelial growth factor) are present in this pathology. Injections of antibodies against VEGF into the vitreous humor of diseased patients have shown to reduce the vessel growth and restore some vision. Unfortunately, numerous injections over time are necessary to create this effect (Ip, Scott et al. 2008). Moreover, individuals with advanced disease, which entails progressive cell death, are not helped by this type of therapy. Photodynamic laser treatment offers another method of reducing blood vessel growth, but once again, irreversible cell death cannot be treated and patients with advanced disease will not benefit from this treatment. There are currently no treatments available to patients with the “dry” AMD (Figuroa, Schocket et al. 2004).

Retinal pigmentosa is another disease that affects the photoreceptors and leads to decreased vision. In this degenerative disease, mutations in the genes that code for the

molecules of the visual cycle cause disturbances in the cycle that lead to apoptosis of photoreceptors (Ferrari, Di Iorio et al.). The goal of the visual cycle is to convert the light entering the eye into an electrical signal which is sent to targets in the brain for processing. If the signal fails to reach the target, vision will be impaired or completely lost. The visual cycle is initiated when light is absorbed by rhodopsin within the photoreceptors. Rhodopsin is a protein that consists of a chromophore and opsin, a membrane protein. The light interaction causes a conformational change in the chromophore from 11-cis-retinal to all-trans-retinal. The change of the chromophore triggers opsin to undergo its own conformational change, which results in the hyperpolarization of the cell. Additionally, the chromophore is released from its bond with opsin, it is reduced to all-trans-retinol, and moves into the retinal pigment epithelium layer of the retina. An enzyme present in this layer, called RPE65, converts the chromophore back to 11-cis-retinal and the cycle can begin again (Purves, Augustine et al. 2001). The majority of cases of retinal pigmentosa are caused by mutations in the gene that code for rhodopsin, and to a lesser extent RPE65 (Ferrari, Di Iorio et al.). High doses of vitamin A slow the progression of the disease. Unfortunately, these levels of vitamin A cause liver damage (Berson, Rosner et al. 1993). Gene therapy is another option for treatment of retinitis pigmentosa. There are studies that show vision can be restored in rodents using adeno-associated virus to deliver correct copies of genes to replace the mutated copies present in this genetic disease (Wert, Davis et al. 2013). These studies are pending FDA approval to move into clinical trials.

Gene therapy and neurotrophic factor treatments offer hope to patients who are early enough in the disease that their photoreceptors have not undergone cell death. Thus

far, there has not been much success investigating potential treatments of advanced age-related macular degeneration or retinitis pigmentosa, in which the photoreceptors have already died. One group attempted to replace damaged photoreceptors with injections of photoreceptor precursor cells (MacLaren, Pearson et al. 2006). Like most transplant studies, there were design challenges related to cell retention and therefore integration of transplanted cells. Also, there was low survival of the photoreceptor precursors. The injected cells that did survive and integrate were able to reach their target and capable of transmitting a downstream signal in response to light. Another study published over five years later, followed a modified protocol to subretinally inject photoreceptor precursors (Pearson, Barber et al.). Although this group was able to achieve increased numbers of integrated cell number by 20-30 times, it was not enough to increase visual function. Due to the low number of integrated cells, neither of these studies was able to show that the transplanted cells increased visual function.

Research on degenerative photoreceptor diseases is limited by the fact that photoreceptors have very poor survival in culture. A better culture system is needed to properly study photoreceptors and their related diseases. Photoreceptors are able to survive better when their natural environment is mimicked with the presence of retinal pigment epithelium. For example, immature mouse photoreceptors are able to mature, survive, and send signals to a target when co-cultured with retinal pigment epithelium (Bandyopadhyay and Rohrer 2010). On the other hand, when a control group of retinas were cultured alone they are unable to form photoreceptor outer segments due to incorrect folding of the proteins that form the discs of these cells. Consequently, these photoreceptors are not functional and cannot play their role in the transduction of light

into an electrical signal. These findings were supported with data that showed that rat neonatal retinal organotypic cultures were able to grow an outer limiting membrane only when cultured in the presence of RPE (Pinzon-Duarte, Kohler et al. 2000). More published data on the subject demonstrated the dependence of photoreceptors on the retinal pigment epithelium (Jacobson, Aleman et al. 2007). Patients with a deficiency in RPE65 are shown to have photoreceptor death and loss of function in the early onset of the disease. RPE65 is the enzyme within the RPE layer that is responsible for converting the photoreceptor's chromophore back into a useable form so that the visual cycle can continue. As seen in this example, without the completion of this conversion the cycle stops, photoreceptors degenerate, and vision is impaired.

Scaffolds alleviate some of the challenges involved in cell delivery and increase the survival and integration of various cell types. Many groups have utilized various types of scaffold systems in order to deliver cells to damaged tissue, such as, cornea (Pang, Du et al.) (Zajicova, Pokorna et al.), myocardium (Wei, Chen et al. 2008) (Xiang, Liao et al. 2006) (Ravichandran, Venugopal et al.), and spinal cord (Chen, Hu et al.) (Xiong, Zhu et al.). Some have even designed novel delivery systems that utilize scaffolds for the delivery of photoreceptor precursors into the retina. One such scaffold was constructed from an elastic polymer, polyglycerol sebacate (PGS) which was seeded with retinal progenitor cells, rolled into cylinder, and injected into the subretinal space through a syringe (Redenti, Neeley et al. 2009). This was achievable because, as a result of the mold and spin coating manufactured process, the scaffold was only 45 microns thick and had pores with an average diameter of 50 microns in which the cells could adhere for safe delivery. Even with this physical protection, very few of the seeded cells

were able to migrate into the host retina. Two hundred and fifty thousand retinal progenitor cells were seeded onto the scaffold, yet only 360-672 of them migrated to the host retina. Nonetheless, *in vivo* experiments showed that the transplanted cells were able to migrate into different layers of the host retina and some of the cells, based on their differentiation, even migrated to the correct layer. Another novel cell encapsulation method was used to better increase retention and to control the transplanted cells orientation, interactions, and migration within the host (Sodha, Wall et al. 2011). Casted thin film polymer sheets that were 10 microns thick and each had different pores sizes. The films were stacked on top of each other and pressure was used to seal them together. The resulting scaffold had an inner chamber with 200 microns pores intended for cell encapsulation and protection. The outer layers had pores of 10 microns or 60 microns and were designed to allow the encapsulated cells to interact with the RPE layer and neural retina, respectively. Further studies are necessary to determine if the design of this scaffold increases transplanted cell retention and migration *in vivo*.

Is there a way to support photoreceptor survival with the presence of RPE and enhance the delivery and retention of transplanted photoreceptors while conserving the natural organization of these two cell types? A two-layered biodegradable polymer scaffold that serves as support and a permeable barrier between photoreceptors and RPE could in fact provide this support and could enhance photoreceptor integration at the target site. Ideally, the first layer of this scaffold would be made of a biodegradable polymer onto which the RPE cells would be cultured. During these design phases of our work, we are using glass for this layer of the scaffold. Another slower degrading polymer would cover the RPE cells and act as a culture surface for seeded photoreceptor

cells. This type of system will increase the survival of the photoreceptors by nurturing their dependence on RPE. Also, this scaffold will increase the efficiency of cell delivery by increasing the availability of the photoreceptors and therefore their chances of integration at the desired site.

Our proposed scaffold enhances the retention of seeded cells because it is composed of a fibrous, electrospun polymer. The electrospinning process creates a porous scaffold that has a high surface to volume ratio, made of nanoscale fibers, that mimics the extracellular matrix (Heydarkhan-Hagvall, Schenke-Layland et al. 2008). These characteristics are beneficial for our application because a permeable scaffold that is similar to the cells' native environment can support cell retention, act as a barrier to protect and encourage compartmentalization of the two cells types, while also permitting the outer segments of the photoreceptors to pass through and interact with the co-delivered retinal pigment epithelium.

How to create this permeable barrier? We hypothesized that an electrospun scaffold might serve this purpose. Electrospinning is a process in which nanoscale fibers are drawn from an electrified solution. This phenomenon was first observed by William Gilbert in 1600 when he noticed droplet formation in water held near an electrified piece of amber. In his 1887 publication, Charles Vernon Boys describes the electrospinning process to form nanofibers. He used shellac, beeswax, and sealing-wax. Then, the shape of the cone that is formed in the droplet before it breaks into stream was mathematically modeled by Sir Geoffrey Ingram Taylor in 1969. Over these years, electrospinning was mainly utilized to manufacture textiles and filters (Tucker, Stanger et al. 2012). More recently, electrospun polymers has been widely used in the medical field to manufacture

a variety of products. Tissue engineers have recognized the advantages of the use of electrospun polymer scaffolds for use in many types of tissue and cell replacement strategies. Some such strategies have resulted in tissue engineered myocardium (Wei, Chen et al. 2008), spinal cord (Zhu, Wang et al. 2010), interfacial tendons and ligaments (Ramalingam, Young et al. 2013), bone (Paletta, Mack et al. 2011), vascular tissue (He, Ma et al. 2009), muscle (Riboldi, Sampaolesi et al. 2005), and cornea (Deshpande, McKean et al.).

The schematic in Figure 4 shows how electrospinning works. Basically, a voltage from a high power source is applied to a polymer exiting the tip of a syringe, which is attached to a syringe pump that is set to a constant rate. When the voltage potential is enough to overcome the viscosity of the polymer, it forms charged particles exiting the tip of the syringe which whip back and forth, and eventually jump to the grounded collector. As the particles whip back and forth in the space between the syringe tip and the collector, the polymer's solvent evaporates and polymer fibers are left behind in a random mat-like orientation on the collector. It is important to choose the most appropriate polymer to electrospin for a given application. For our proposed scaffold, we wanted a biocompatible polymer that slowly degrades over time at a known rate. This enables the scaffold to provide support for the photoreceptors and RPE when they are initially transplanted and then dissipate over time as the cells become integrated in the native retinal tissue. The continued presence of the scaffold would not be needed and may in fact inhibit further integration. Polyesters are often the material chosen for biodegradable scaffolds because their degradation rates and biocompatibility have been widely studied (Pitt and Gu 1987). For our application, polylactic acid, or PLA, was

chosen because of its well understood slow degradation. PLA is part of a group of poly-a-hydroxyesters that have been produced for over 30 years. As biodegradable polyesters are hydrolyzed, they create byproducts that can cause the culture media to become acidic. The hydrolysis of polyesters causes the polymer to become more brittle, eventually leading to bulk erosion and loss of performance over time. All polyesters undergo this reaction with aqueous solutions, but the rate of degradation can be altered by culture temperature, molecular structure, the density of the ester groups, and the type of aqueous solution used. For example, due to its molecular structure, PGA is hydrophilic which leads to a high degradation rate (6-12 months). On the other hand, PLA is hydrophobic so it degrades slower (12-16 months) (Vieira, Vieira et al. 2009). Also, the byproducts of PLA's slow degradation will not negatively affect the integrity of the scaffold itself or its associated cells (Sung, Meredith et al. 2004).

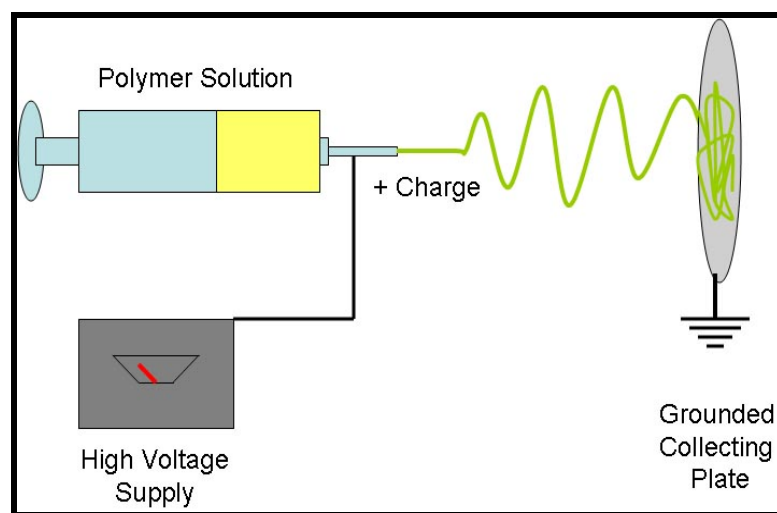


Figure 4 – Schematic of electrospinning process (Diagram by K Kador, unpublished)

The benefits of the use of electrospun polymers for retinal cell replacement are already being studied by many. One such study seeded retinal progenitor cells onto scaffolds that were electrospun with different ratios of PCL and chitosan (Chen, Fan et al. 2011). The scaffolds that were produced had fiber diameters between 656nm and 925nm and porosity between 77%-89%. When compared to the control tissue culture plate, the scaffolds were able to better support the cells. Furthermore, the scaffold enhanced cell proliferation and differentiation towards a neuronal phenotype. Another study went a few steps further and seeded an electrospun PCL scaffold with retinal progenitor cells for *ex vivo* experiments (Cai, Smith et al. 2011). They reported that their PCL scaffolds were 15 microns thick, average fiber diameter of about 3 microns, 52% porosity, and an average pore size of 24.4 microns. The seeded cells were able to proliferate and extend processes on top of the scaffold and into its pores. *Ex vivo* experiments, in which the cells were cultured with explanted retinas, showed that the seeded progenitor cells were able to migrate through the porous scaffolds into the retinal layers of explants from wild-type and disease-state mice. Some of the migrating cells and some of the cells that remained on the scaffold expressed markers for retinal neurons and photoreceptors, NF200 and rhodopsin, respectively. Moreover, a few of the rhodopsin positive cells migrated to the outer nuclear layer of the retina. *In vivo* experiments are necessary to determine if transplanted cells from this system can increase visual function.

Even though other studies have utilized various scaffolds to support either photoreceptors or their precursor cells, none of these studies co-delivered RPE cells. This novel co-delivery is possible because we electrospun polylactic acid fibers on top of living RPE cells and seeded photoreceptors on top of the fibers. The mechanical

properties of the polymer fibers enable them to provide the support needed to keep the photoreceptors separate from the RPE cells, while the porosity of the scaffold allows for filtration and interaction between the two cell types. We used scanning electron microscopy, a Live/Dead cell assay, and immunohistochemistry to prove our hypothesis that it is possible to electrospin PLA scaffolds with consistent fiber diameters on top of living RPE cells, the cells are able to recover and display the same viability as control samples, and the scaffolds provide the support necessary for the seeded photoreceptors to remain separated and above the RPE layer, as found in natural retina.

Chapter 2: Methods

Isolation and Culturing of Retinal Pigment Epithelium

The Lions Eye Bank at Bascom Palmer Eye Institute provided human eyes for dissection. The RPE was isolated as described by others (Blenkinsop, Salero et al. 2013) and the cells were cultured using a modified protocol. Briefly, the RPE layer was obtained by removing the vitreous and retina, rinsing with PBS (Gibco), and adding cell dissociation Hank's buffer (Gibco) directly into the eyecup for 10 minutes at 37 degrees C. The buffer was then replaced with DMEM/F12 (Gibco) supplemented with 20% FBS and a spatula was used to scrape 1 mm sheets of RPE from the Bruch's membrane. The sheets were collected in a 15 ml falcon tube where a sucrose gradient separated single cells from sheets of RPE. They were then plated onto 6-well tissue culture plates which were lined with glass cover slips. To promote cell adhesion the coverslips were treated with poly-D lysine for 30 minutes and laminin overnight in 10% CO₂ at 37 degrees. The sheets were cultured in RPE until a cobblestone monolayer of cells was seen under light microscopy to be at about 70% confluence. The RPE cells from pig and mouse were previously harvested from these species following the same protocol as above, then frozen in DMSO, and stored in liquid nitrogen. The cells were thawed when needed and cultured as described above.

Electrospinning PLA on top of Retinal Pigment Epithelium

After the RPE cells were confluent and covered the entire glass coverslip, the coverslips were carefully removed from their media with forceps and placed on the collector of the electrospinning setup with the cell-coated side facing up. The grounded collector stand is

circular and has a diameter smaller than the circular coverslip. The system was designed in such a way so that the some of electrospun fibers would wrap underneath the coverslip. Poly D, L Lactic acid (Purac Biochem) was dissolved in HFIP (Chem-Impex International Inc) to make a 6.6% solution. A glass syringe was filled with the PLA solution and placed in continuous rate syringe pump (New Era Pump Systems). The vertical distance between the collector stand and the tip of the electrified Hamilton 20 gauge needle was 12 cm. The needle was connected to a voltage power supply (Spellman HV 230-30R) set to 15 kV. Computer software was used to control the volume of polymer and deliver it at the specified rate. In these experiments, 30 microliters of PLA was delivered at 2 ml/hr for each run. These parameters were determined based on previously published (Kador, Montero et al. 2013) and unpublished data from our lab. Kador et al tested various parameters to determine which were optimal for PLA electrospun fibers. These parameters result in an average fiber diameter of 0.5 microns with random mat-like orientation. After the syringe pump stopped, the voltage source was turned off and the coverslip was carefully removed from the collector stand with the use of a clean scalpel. Then, the coverslip was flipped over and placed securely on the collector stand with the cell-coated side down. The bottom of the coverslip was coated with a double layer of PLA by performing two sequential runs with the same parameters as above. This was to ensure the coverslip was securely wrapped with fibers, but proper filtration could still occur for the cells on the top of the coverslip. It should also be noted that since living cells were used, the equipment and tools that come into contact with the living cells were sterilized with ethanol or UV light. After both sides of the coverslip were coated with PLA fibers, the completed scaffold was removed from the collector

stand and placed back in RPE media in a 12-well plate. The cells were allowed to recover for 5 days in the incubator at 5% CO₂/ 37 degrees C.

Live/Dead Assay of RPE after Electrospinning

In some experiments, a group of scaffolds were removed from culture after 2 days and a Live/Dead viability assay was performed. The survival of the RPE cells that were covered with PLA fibers was compared to the survival of a control group of cells that were also cultured on glass coverslips, but did not undergo the electrospinning process. The assay was performed by adding Calcein AM and Propidium Iodide (Invitrogen) into the culture media at a dilution of 1:1000 for 15 minutes at 5% CO₂/ 37 degrees C. After changing to fresh media, the culture was imaged under confocal microscopy (Leica TCS SP5) and quantified with ImageJ software. Calcein AM labels the cytoplasm of living cells with green fluorescence because of a reaction that occurs with estrases within the cells. On the other hand, Propidium Iodide cannot enter cells but it causes a reaction with nucleic acids on the membranes of compromised cells to label them red.

Scanning Electron Microscopy of RPE/PLA Scaffold

To analyze the fiber diameter, a group of scaffolds were imaged by environmental scanning electron microscopy. Samples were sputter coated with gold and imaged at 500x and 5000x magnification under high vacuum using a FEI XL-30 Field Emission Environmental SEM. This low vacuum, aqueous environment SEM was chosen to preserve the actual pore sizes and fiber diameters of the scaffolds. The average fiber diameter was determined by measuring 15 fibers from 3 regions of interest of 3 scaffolds.

Harvesting an Enriched-Photoreceptor Retinal Suspension and Seeding onto RPE/PLA Scaffold

Retina was isolated from early postnatal rats and processed to obtain an enriched photoreceptor retinal suspension. The isolation was performed as described previously with some modifications (Goldberg, Klassen et al. 2002). Briefly, the harvested retinas were digested in papain (Worthington Biochemicals) and mechanical titration was used to dissociate the cells into a single suspension. Dishes were coated with antibodies raised against the various cells types of the retina (Jackson Immunolabs). The macrophages, retinal ganglion cells, and amacrine cells were removed by pouring the retinal suspension from one antibody-coated plate to the next. The final cell suspension was collected in a conical tube and is considered to be enriched with photoreceptors. This suspension was centrifuged at 80 g for 15 minutes and re-suspended in Neurobasal media supplemented with insulin (Sigma), sodium pyruvate (Sigma), penicillin/streptomycin (Sigma), n-acetyl cysteine (Sigma), triiodo-thyronine (Sigma), forskolin (Sigma), Sato, B27 and BDNF (Peprotech) and CNTF (Peprotech) growth factors. The photoreceptor enriched retinal suspension was then seeded on top of the electrospun fibers of the scaffolds and cultured together with the RPE cells for another 3 days at 5% CO₂/37 degrees C.

Immunohistochemistry

The scaffold samples that underwent immunohistochemistry were first fixed with 4% paraformaldehyde (Electron Microscopy Services) in PBS (Gibco). Then, they were permeabilized with Triton X and blocked with 10% normal goat serum (Sigma). The samples were stained with recoverin (Sigma), a rabbit polyclonal antibody, to visualize the photoreceptors and GFP, a chicken monoclonal antibody (Invitrogen), to enhance the

GFP signal from the lenti-virus infected RPE cells. Both primary antibodies were used at a dilution of 1:500 and incubated overnight at 4 degrees Celsius. The next day the samples were washed three times with PBS before the addition of the secondary antibodies. AlexaFluor 488 goat anti-chicken (Invitrogen) and AlexaFluor 546 goat anti-rabbit (Invitrogen) were added to samples at a dilution of 1:1000 and incubated for 30 minutes at room temperature. The secondary antibodies were removed with three washes of PBS. DAPI was added at a dilution of 1:5000 into the second wash in order to stain all cell nuclei. Finally, the samples were imaged under confocal microscopy (Leica TCP SP5).

Chapter 3: Results

Electrospun PLA Fiber Size

The electrospinning method consistently produced PLA fibers with an average diameter of about 500 microns that formed mat-like scaffolds with random fiber orientation. The parameters chosen to create the fibers were based on previously published data from our lab shows that consistent fiber diameters of about 500 microns can be electrospun when 15 kilovolts is applied to a syringe tip 12 centimeters from the grounded collector and set to a rate of 2 mL/hour (Figure 5). Higher voltages resulted in fibers that were too thin for this application, while lower voltages produced misshaped fibers with bead formations.

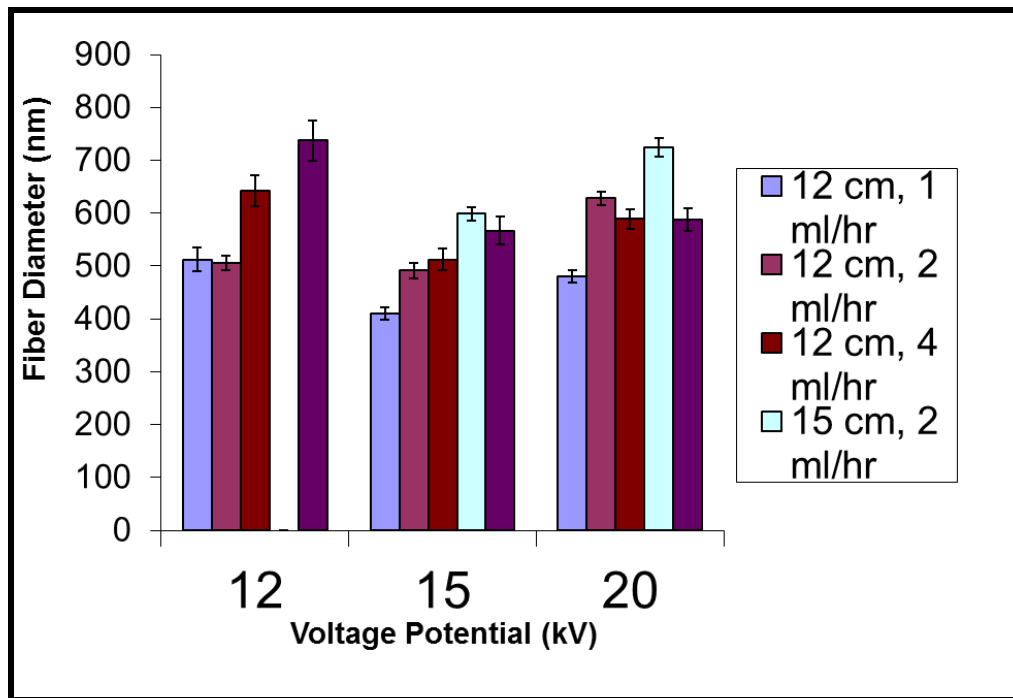


Figure 5 – Electrospinning parameter variations and resulting fiber diameters

RPE Survival after Electrospinning

The first step in developing this scaffold was to ensure that it was possible to electrospin on top of living cells and for them to survive. SEM images of the scaffolds showed that the RPE cells appeared to be beneath the electrospun PLA fibers (Figure 6). Moreover, fluorescence microscopy revealed that based on cell morphology and GFP expression, the RPE cells were still alive after two days underneath the fibers (Figure 7). When the scaffold was pulled away, it was possible to visualize the basement layer of RPE cells (Figure 8). The RPE were able to maintain their cobble-stone morphology and appear to form gap junctions with other neighboring RPE cells. The viability of the RPE cells post electrospinning was also demonstrated by the cells' ability to proliferate to near confluence under the scaffold. Initially, GFP-positive RPE cells were cultured on glass cover slips and PLA fibers were spun on top while they were at about 70% confluence (Figure 9a). After five days in culture, the cells were able to reach nearly 100% confluence (Figure 9b).

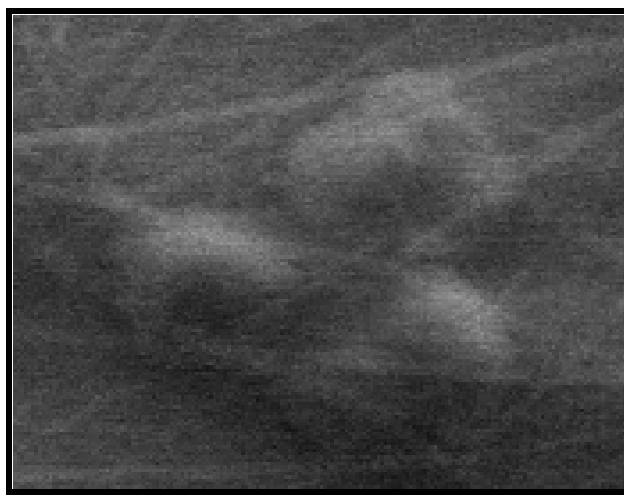


Figure 6 – SEM of cultured RPE Cells beneath PLA fibers

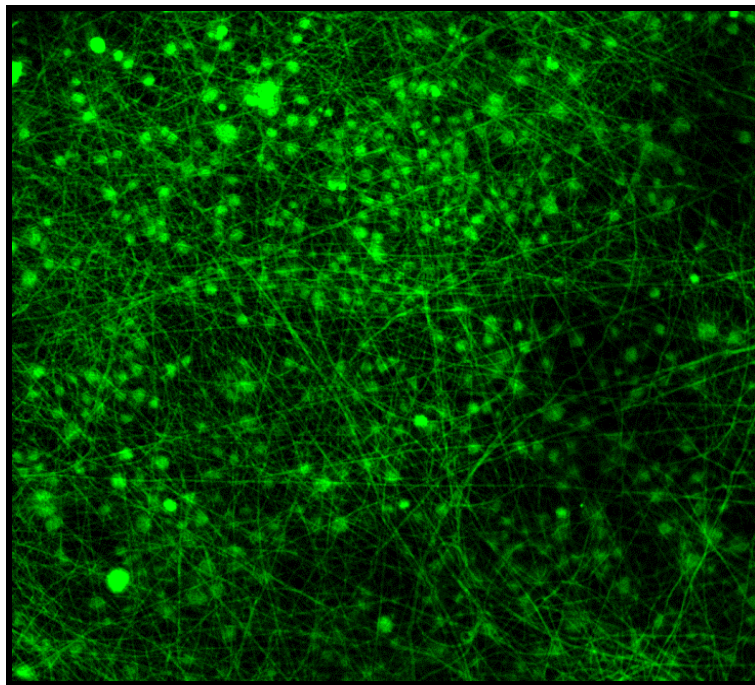


Figure 7 – Fluorescence microscopy of GFP- positive RPE Cells beneath PLA fibers

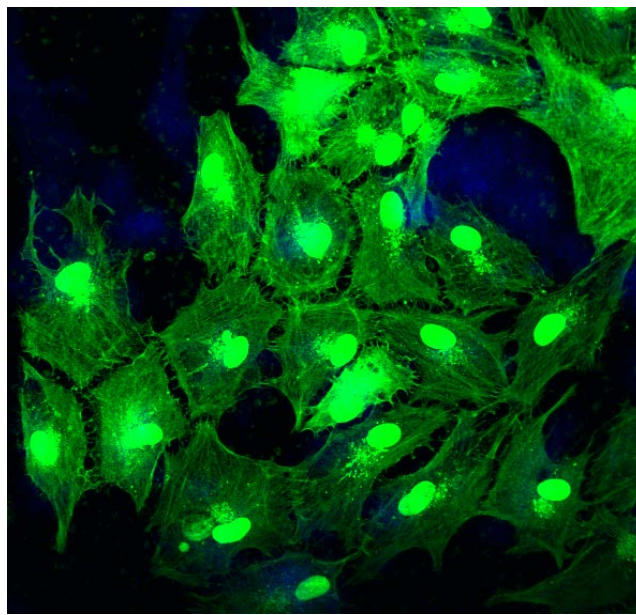


Figure 8 – Confocal microscopy of RPE Cells with scaffold removed

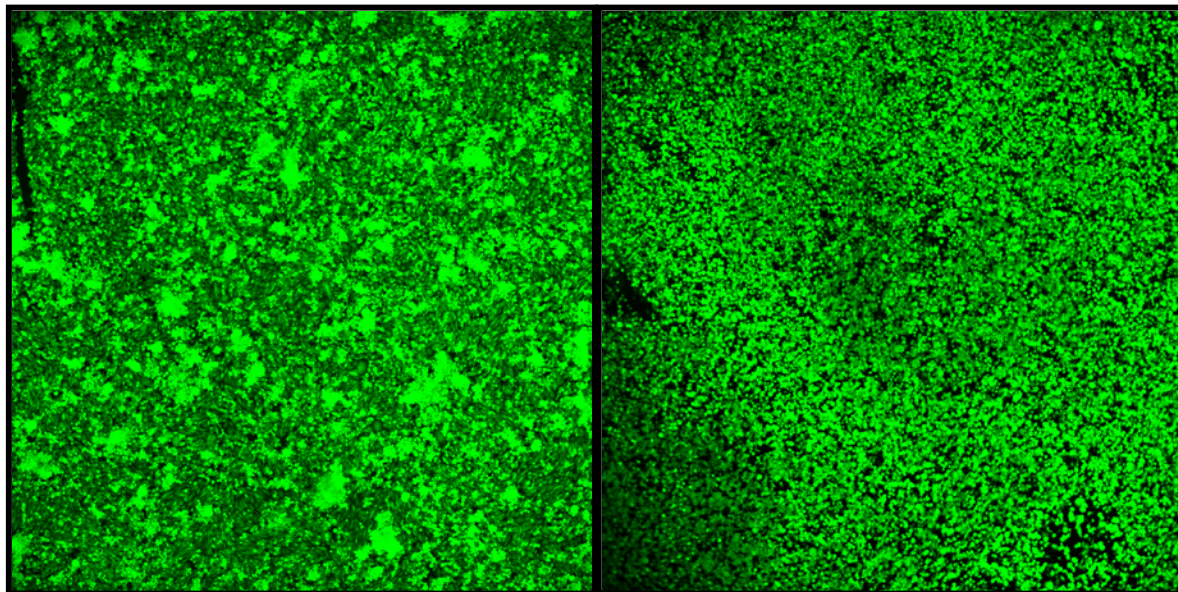


Figure 9 – Fluorescence microscopy of RPE confluence under fibers after one day in culture (a) and 5 days (b)

In order to quantify the viability of the RPE cells, a Live/Dead Assay was performed on a group of scaffolds after two days in culture post electrospinning. This time point was selected because if the cells were given more time in culture, they may have been able to completely recover from the stress of electrospinning. Therefore, the two day time point provides a better measure of the effect of electrospinning on the viability of the cells. The results of the assay showed that there was no significant difference between the survival of the cells covered with electrospun PLA fibers compared to the control group of cells that did not undergo electrospinning (Figure 10). Therefore, we were able to electrospin PLA fibers onto living RPE cells which are able to survive and continue to grow at rates similar to controls.

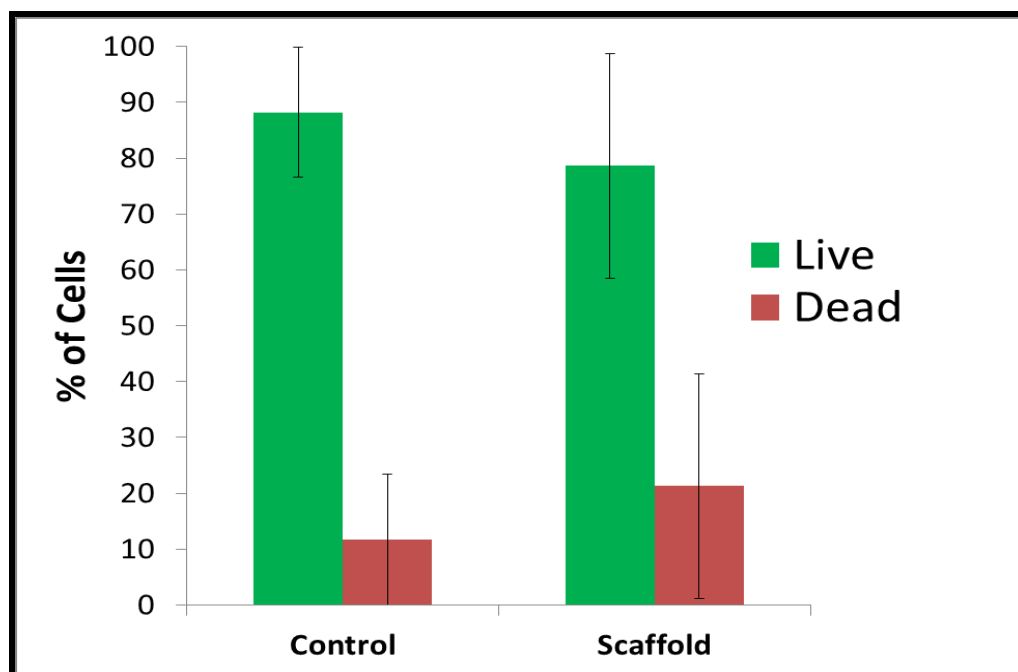


Figure 10 – Live Dead Assay of RPE after Electrospinning

RPE and Photoreceptor Separation

The PLA fibers between the RPE and photoreceptor layers must act as a barrier to keep the cells separated in their native orientation, but still allow the cells to interact. The photoreceptors will not survive or function normally in culture without interactions with RPE. This is the reason why this scaffold was designed to support both cell types. After being seeded on top of the fibers and cultured for five days, the photoreceptors appeared to reside above the RPE layer which is beneath the PLA fibers. The separation of the cell types was visualized under confocal microscopy by labeling the photoreceptors with an antibody against recoverin and subsequently a fluorescently tagged secondary antibody. Since the RPE cells were cultured in GFP-lentivirus, those cells can be identified by GFP expression. Velocity confocal imaging of the scaffolds revealed that the red photoreceptors appear to be above the green RPE layer (Figure 11). The

separation is more apparent when the same velocity image is rotated to visualize the z-plane (Figure 12) and compared to a control sample (Figure 13). The photoreceptors and RPE cells of the control samples do not have a barrier between them and therefore cannot keep their native orientation. In order to quantify the separation of these cells, we measured the fluorescent intensity of the wavelengths that correspond with the emission spectra of the secondary antibodies used to label the two different cells types. This measurement was plotted as a function of its position along the z-axis for the scaffold and control samples (Figures 14 and 15). In general, the position in which a group of fluorescent cells is located is where its characteristic wavelength is emitted most intensely. The photoreceptors and RPE cells on the scaffold samples had distinct, separate peaks of fluorescent intensity that did not overlap along the z-axis. In contrast, the fluorescent intensity peak of the RPE cells in the control samples almost completely overlapped the peak of the photoreceptors along the z-axis. This indicated that the photoreceptors in the control samples are not lying above the RPE cells, but instead they had fallen in between them.

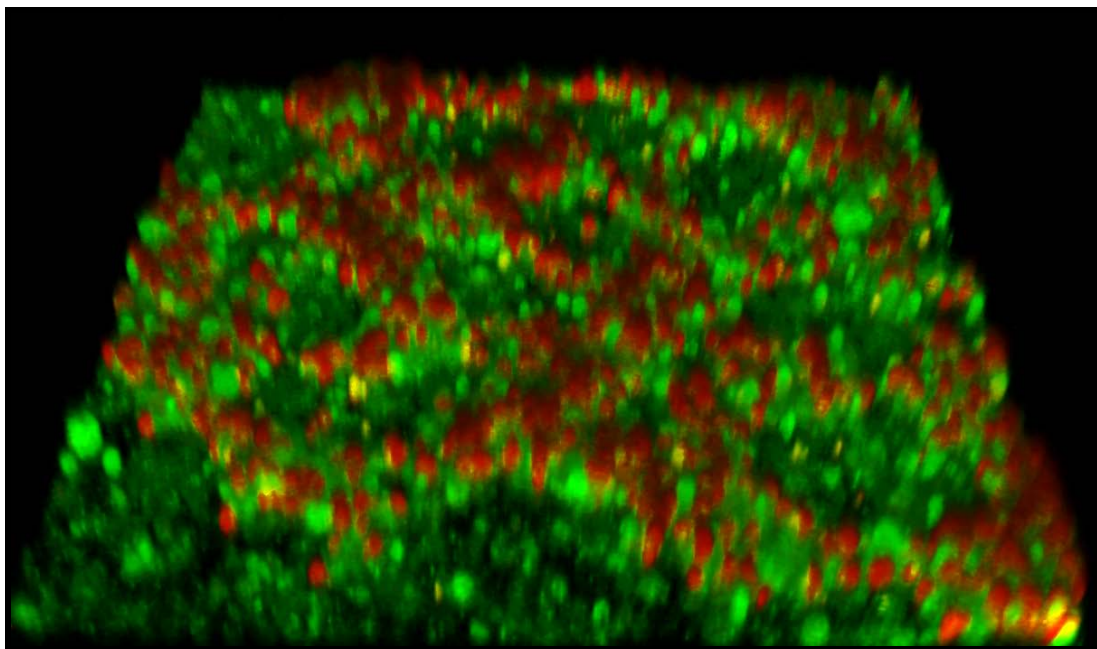


Figure 11 – Velocity confocal image above scaffold with recoverin-positive photoreceptors and GFP-positive RPE cells

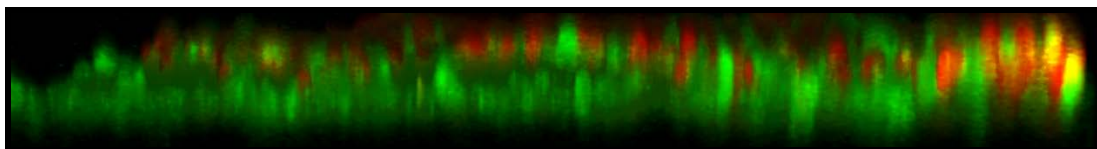


Figure 12 – Cross section through z-axis of above image

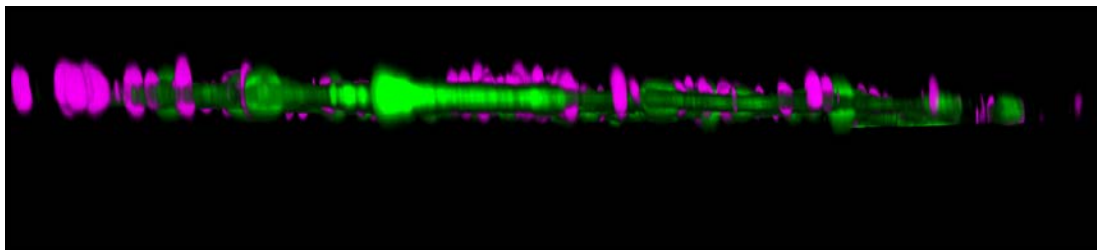


Figure 13 – Cross section through z-axis of control sample

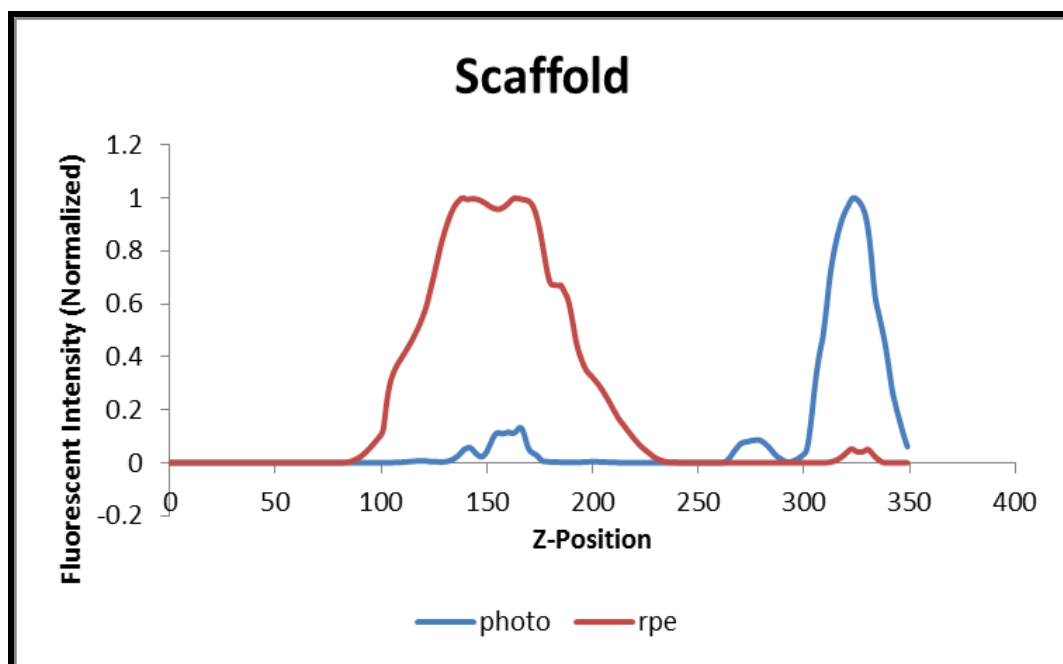


Figure 14 – Measurement of fluorescence emitted from photoreceptors and RPE along the z-axis of a scaffold sample

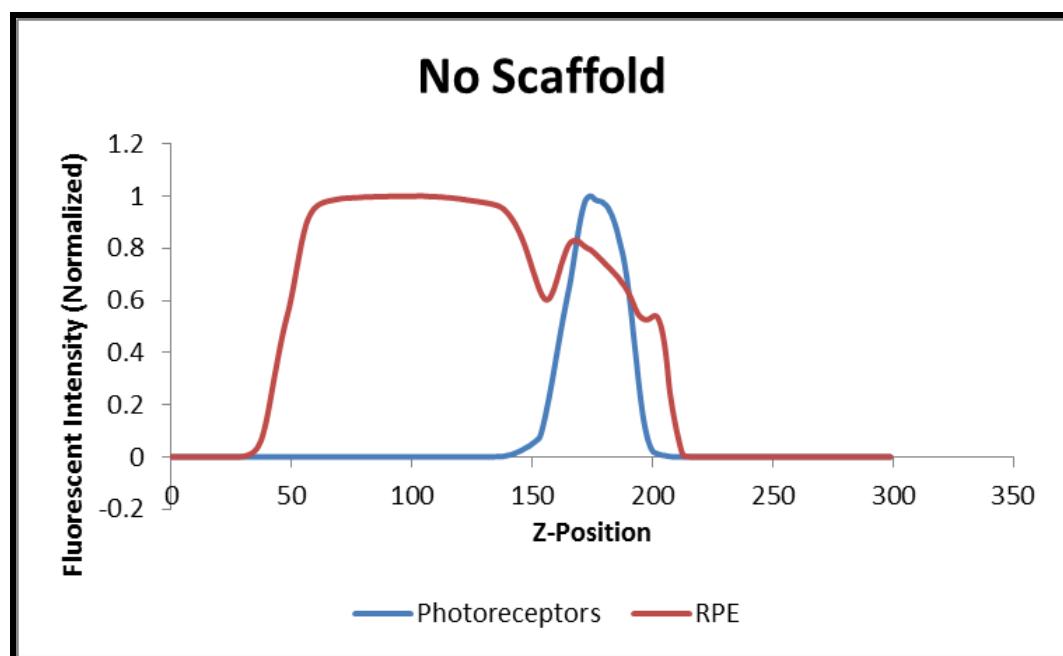


Figure 15 – Measurement of fluorescence emitted from photoreceptors and RPE along the z-axis of a control sample

Further analysis was performed to enumerate the separation of the two cell types. The z-position of the peak emission of the photoreceptors was subtracted from the z-position of the peak emission of the RPE cells to determine the z-separation between the two cell types (Figure 16). This analysis shows that the scaffold allowed for the cells to be on average about 3 times more separated when compared to the control. Furthermore, several confocal images were captured that show the outer segments of recoverin-positive photoreceptors that extended towards the RPE layer. (Figures 17 and 18) This was an important finding because for the scaffold to function properly, it must act as a barrier but not prevent the cells from interacting. Therefore, we have created a scaffold that is able to support seeded photoreceptors, keep them separated from an underlying RPE layer, while still allowing them to extend their outer segments towards the RPE layer

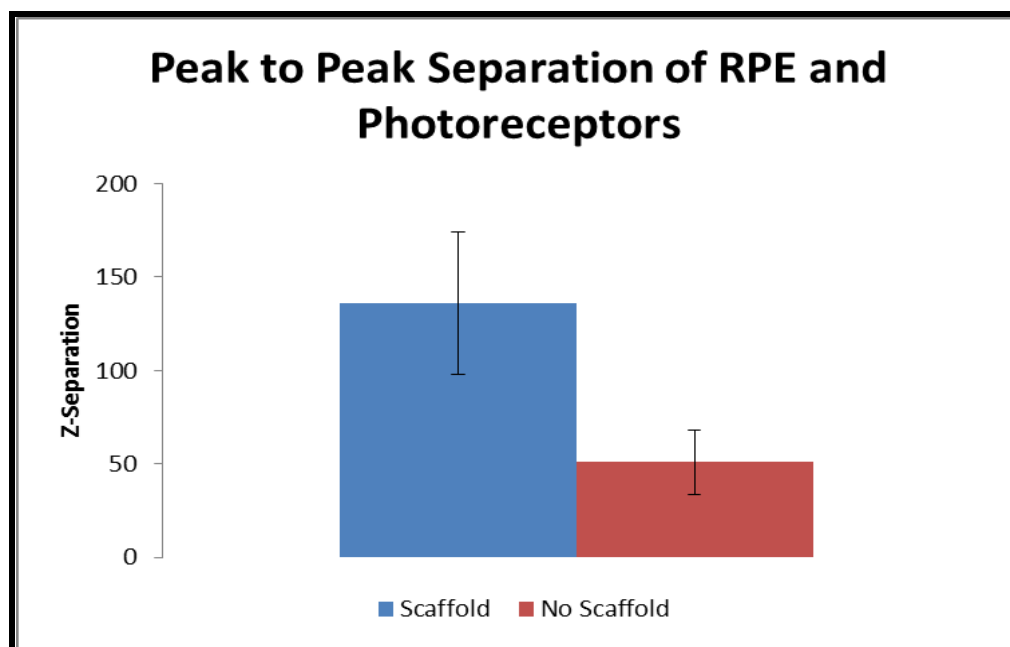


Figure 16 – Quantification of the separation of photoreceptors and RPE along the z-axis of scaffold and control samples

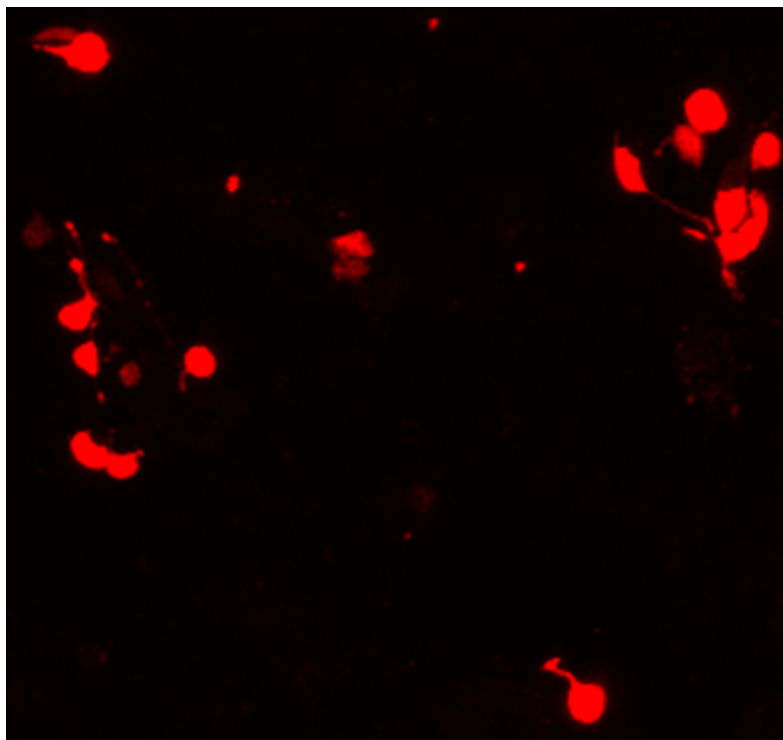


Figure 17 – Recoverin-positive photoreceptors with outer segments extending downward in scaffold sample (Scale Bar 10X)

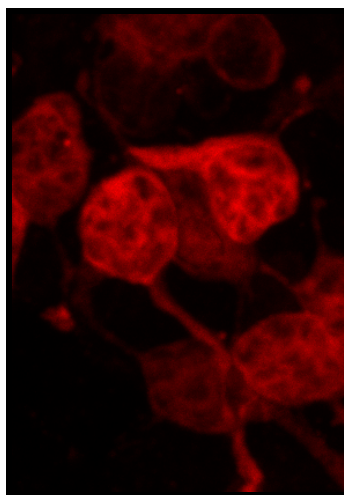


Figure 18 – Recoverin-positive photoreceptors with outer segments extending downward in scaffold sample (Scale Bar 40X)

Chapter 4: Discussion

Here we work towards a three-dimensional scaffold for photoreceptor-RPE tissue engineering and eventual cell delivery. In these experiments, we demonstrated that it is possible to electrospin uniform PLA fibers into an average diameter of 500 nm onto living RPE cells which are able to remain viable. This is important because if the fibers were too thin or too sparse, the gaps in between them would be large enough for the subsequently seeded photoreceptors to fall through to the RPE layer and the two cell types will not be separated as desired. If the fibers were too large, they would not allow for filtration and possibly block the necessary interactions between the RPE and the photoreceptors. The size and random mat-like orientation of the PLA fibers enabled the scaffold to support the seeded photoreceptors.

To our knowledge, there are no other studies that use an electrospun scaffold for photoreceptor seeding and culture. There is a recent study in which the investigators seeded MSCs onto electrospun scaffolds with fiber diameters similar to our scaffold's fiber diameter (Nadri, Kazemi et al. 2013). The MSCs that were seeded on top of randomly oriented fibers were more likely to differentiate into photoreceptors than MSCs seeded onto aligned fibers or tissue culture plates. This indicates that photoreceptors may prefer a surface for growth that has randomly oriented fibers of this size and supports our findings that our scaffold was able to support photoreceptors in culture. Photoreceptors may be preferential to this type of surface because it mimics the extracellular matrix. A primary component of the ECM is collagen fibrils with diameters in the nanometer and submicron range (Bear, Connors et al. 2001).

To date, no other groups have published scaffold designs that utilize the electrospinning process to collect fibers directly on top of living cells. There are some groups that incorporated cells into the polymer fibers by spraying the cells onto scaffolds as they materialized (Seil and Webster 2011). Other groups co-spun solutions of cells along with their polymer solutions with the assistance of a coaxial spinneret (Townsend-Nicholson and Jayasinghe 2006) (Paletta, Mack et al. 2011). One such group electrospayed osteoblasts while electrospinning PLLA in parallel. However, the survival of the cells and the structure of the scaffolds were both affected by the processes. This is not surprising considering the shear stresses that must have been exerted on these cells. The RPE cells underneath the fibers of our scaffold were not only able to grow to confluence, but were assayed to be as viable as control cells. These findings could assist in the development of biodegradable scaffolds of tissues that were previously challenging to model due to their multi-layered, highly structured architecture.

We also showed that our electrospun scaffold is able to act as a permeable barrier to separate seeded photoreceptors from RPE cells below the scaffold, while still allowing them to extend their outer segments through the scaffold to the RPE layer. It was important to keep the two cell types separated by a permeable barrier so that the cells could interact and exchange signals without sacrificing their natural compartmentalization. Also, as previously mentioned, photoreceptors do not survive well in culture if RPE cells are not present (Bandyopadhyay and Rohrer 2010) (Jacobson, Aleman et al. 2007). This is a major challenge for in vitro photoreceptor research. Since our scaffold is designed to co-deliver RPE cells, it can provide a better modeling system to study various photoreceptor diseases and treatments. Furthermore, following

additional developments our scaffold could be used to replace degenerated photoreceptors in patients with AMD and retinitis pigmentosa.

Chapter 5: Conclusion

In conclusion, we have proven that it is possible to electrospin PLA scaffolds with consistent fiber diameters on top of living RPE cells, the cells are able to recover and display the same viability as control samples, and the scaffolds provide the support necessary for the seeded photoreceptors to remain separated and above the RPE while still allowing them to extend their outer segments downward. Future aims of this work include replacing the glass surface that supports the RPE layer with a second biodegradable polymer. It will also be important to show that the photoreceptors in our system are still light responsive. This could be accomplished with electrophysiology. Next, it will be necessary to assure that the RPE and the photoreceptors are able to function naturally in our system. This could be demonstrated by the RPE cells' ability to phagocytosis the outer segments of the photoreceptors. Lastly, a final goal of this work is the in vivo transplantation of our scaffold into a rodent model to determine if the scaffold can enhance photoreceptor integration and restore visual function in models in which these cells have degenerated.

References

- Bandyopadhyay, M. and B. Rohrer (2010). "Photoreceptor structure and function is maintained in organotypic cultures of mouse retinas." Mol Vis **16**: 1178-1185.
- Bear, M. F., B. W. Connors and M. A. Paradiso (2001). Neuroscience: Exploring the Brain. Baltimore, MD, Lippincott, Williams, and Wilkins.
- Berson, E. L., B. Rosner, M. A. Sandberg, K. C. Hayes, B. W. Nicholson, C. Weigel-DiFranco and W. Willett (1993). "A randomized trial of vitamin A and vitamin E supplementation for retinitis pigmentosa." Arch Ophthalmol **111**(6): 761-772.
- Blenkinsop, T. A., E. Salero, J. H. Stern and S. Temple (2013). "The culture and maintenance of functional retinal pigment epithelial monolayers from adult human eye." Methods Mol Biol **945**: 45-65.
- Cai, S., M. E. Smith, S. M. Redenti, G. E. Wnek and M. J. Young (2011). "Mouse Retinal Progenitor Cell Dynamics on Electrospun Poly(varepsilon-Caprolactone)." J Biomater Sci Polym Ed.
- Chen, G., Y. R. Hu, H. Wan, L. Xia, J. H. Li, F. Yang, X. Qu, S. G. Wang and Z. C (2010). Wang "Functional recovery following traumatic spinal cord injury mediated by a unique polymer scaffold seeded with neural stem cells and Schwann cells." Chin Med J (Engl) **123**(17): 2424-2431.
- Chen, H., X. Fan, J. Xia, P. Chen, X. Zhou, J. Huang, J. Yu and P. Gu (2011). "Electrospun chitosan-graft-poly (varepsilon-caprolactone)/poly (varepsilon-caprolactone) nanofibrous scaffolds for retinal tissue engineering." Int J Nanomedicine **6**: 453-461.
- Deshpande, P., R. McKean, K. A. Blackwood, R. A. Senior, A. Ogunbanjo, A. J. Ryan and S. MacNeil "Using poly(lactide-co-glycolide) electrospun scaffolds to deliver cultured epithelial cells to the cornea." Regen Med. 2010 May;5(3):395-401. doi: 10.2217/rme.10.16.
- Ferrari, S., E. Di Iorio, V. Barbaro, D. Ponzin, F. S. Sorrentino and F. Parmeggiani (2011). "Retinitis pigmentosa: genes and disease mechanisms." Curr Genomics **12**(4): 238-249.
- Figuroa, M., L. S. Schocket, J. DuPont, T. I. Metelitsina and J. E. Grunwald (2004). "Effect of laser treatment for dry age related macular degeneration on foveolar choroidal haemodynamics." Br J Ophthalmol **88**(6): 792-795.
- Goldberg, J. L., M. P. Klassen, Y. Hua and B. A. Barres (2002). "Amacrine-signaled loss of intrinsic axon growth ability by retinal ganglion cells." Science **296**(5574): 1860-1864.

- He, W., Z. Ma, W. E. Teo, Y. X. Dong, P. A. Robless, T. C. Lim and S. Ramakrishna (2009). "Tubular nanofiber scaffolds for tissue engineered small-diameter vascular grafts." J Biomed Mater Res A **90**(1): 205-216.
- Heydarkhan-Hagvall, S., K. Schenke-Layland, A. P. Dhanasopon, F. Rofail, H. Smith, B. M. Wu, R. Shemin, R. E. Beygui and W. R. MacLellan (2008). "Three-dimensional electrospun ECM-based hybrid scaffolds for cardiovascular tissue engineering." Biomaterials **29**(19): 2907-2914.
- Ip, M. S., I. U. Scott, G. C. Brown, M. M. Brown, A. C. Ho, S. S. Huang and F. M. Recchia (2008). "Anti-vascular endothelial growth factor pharmacotherapy for age-related macular degeneration: a report by the American Academy of Ophthalmology." Ophthalmology **115**(10): 1837-1846.
- Jacobson, S. G., T. S. Aleman, A. V. Cideciyan, E. Heon, M. Golczak, W. A. Beltran, A. Sumaroka, S. B. Schwartz, A. J. Roman, E. A. Windsor, J. M. Wilson, G. D. Aguirre, E. M. Stone and K. Palczewski (2007). "Human cone photoreceptor dependence on RPE65 isomerase." Proc Natl Acad Sci U S A **104**(38): 15123-15128.
- Kador, K. E., R. B. Montero, P. Venugopalan, J. Hertz, A. N. Zindell, D. A. Valenzuela, M. S. Uddin, E. B. Lavik, K. J. Muller, F. M. Andreopoulos and J. L. Goldberg (2013). "Tissue engineering the retinal ganglion cell nerve fiber layer." Biomaterials **34**(17): 4242-4250.
- MacLaren, R. E., R. A. Pearson, A. MacNeil, R. H. Douglas, T. E. Salt, M. Akimoto, A. Swaroop, J. C. Sowden and R. R. Ali (2006). "Retinal repair by transplantation of photoreceptor precursors." Nature **444**(7116): 203-207.
- Margalit, E. and S. R. Sadda (2003). "Retinal and optic nerve diseases." Artif Organs **27**(11): 963-974.
- Nadri, S., B. Kazemi, M. B. Eeslaminejad, S. Yazdani and M. Soleimani (2013). "High yield of cells committed to the photoreceptor-like cells from conjunctiva mesenchymal stem cells on nanofibrous scaffolds." Mol Biol Rep.
- Paletta, J., F. Mack, H. Schenderlein, C. Theisen, J. Schmitt, J. Wendroff, S. Agarwal, s. Fuchs-Winkelmann and M. Schofer (2011). "Incorporation of osteoblasts into 3D nanofibre matrices by simultaneous electrospinning and spraying in bone tissue engineering." European Cells and Materials **21**: 384-395.
- Pang, K., L. Du and X. Wu (2010). "A rabbit anterior cornea replacement derived from acellular porcine cornea matrix, epithelial cells and keratocytes." Biomaterials **31**(28): 7257-7265.

Pearson, R. A., A. C. Barber, M. Rizzi, C. Hippert, T. Xue, E. L. West, Y. Duran, A. J. Smith, J. Z. Chuang, S. A. Azam, U. F. Luhmann, A. Benucci, C. H. Sung, J. W. Bainbridge, M. Carandini, K. W. Yau, J. C. Sowden and R. R. Ali (2012). "Restoration of vision after transplantation of photoreceptors." Nature **485**(7396): 99-103.

Pinzon-Duarte, G., K. Kohler, B. Arango-Gonzalez and E. Guenther (2000). "Cell differentiation, synaptogenesis, and influence of the retinal pigment epithelium in a rat neonatal organotypic retina culture." Vision Res **40**(25): 3455-3465.

Pitt, C. and Z.-w. Gu (1987). "Modification of the rates of chain cleavage of polycaprolactone and related polyesters in the solid state." Journal of Controlled Release **4**: 283-292.

Purves, D., G. Augustine, D. Fitzpatrick, L. Katz, A.-S. LaMantia, J. McNamara and W. S. Mark (2001). Neuroscience, Sinauer Associates.

Ramalingam, M., M. F. Young, V. Thomas, L. Sun, L. C. Chow, C. K. Tison, K. Chatterjee, W. C. Miles and C. G. Simon, Jr. (2013). "Nanofiber scaffold gradients for interfacial tissue engineering." J Biomater Appl **27**(6): 695-705.

Ravichandran, R., J. R. Venugopal, S. Sundarrajan, S. Mukherjee and S. Ramakrishna (2011). "Poly(Glycerol sebacate)/gelatin core/shell fibrous structure for regeneration of myocardial infarction." Tissue Eng Part A **17**(9-10): 1363-1373.

Redenti, S., W. L. Neeley, S. Rompani, S. Saigal, J. Yang, H. Klassen, R. Langer and M. J. Young (2009). "Engineering retinal progenitor cell and scrollable poly(glycerol-sebacate) composites for expansion and subretinal transplantation." Biomaterials **30**(20): 3405-3414.

Riboldi, S. A., M. Sampaolesi, P. Neuenschwander, G. Cossu and S. Mantero (2005). "Electrospun degradable polyesterurethane membranes: potential scaffolds for skeletal muscle tissue engineering." Biomaterials **26**(22): 4606-4615.

Roberts, D. (2006). Age-Related Macular Degeneration, Da Capo Press.

Seil, J. T. and T. J. Webster (2011). "Spray deposition of live cells throughout the electrospinning process produces nanofibrous three-dimensional tissue scaffolds." Int J Nanomedicine **6**: 1095-1099.

Sodha, S., K. Wall, S. Redenti, H. Klassen, M. J. Young and S. L. Tao (2011). "Microfabrication of a three-dimensional polycaprolactone thin-film scaffold for retinal progenitor cell encapsulation." J Biomater Sci Polym Ed **22**(4-6): 443-456.

Sung, H. J., C. Meredith, C. Johnson and Z. S. Galis (2004). "The effect of scaffold degradation rate on three-dimensional cell growth and angiogenesis." Biomaterials **25**(26): 5735-5742.

- Townsend-Nicholson, A. and S. N. Jayasinghe (2006). "Cell electrospinning: a unique biotechnique for encapsulating living organisms for generating active biological Microthreads/Scaffolds." Biomacromolecules **7**(12): 3364-3369.
- Tucker, N., J. Stanger, M. Staiger, H. Razzaq and K. Hofman (2012). "The History of the Science and Technology of Electrospinning from 1600-1995." Journal of Engineered Fibers and Fabrics.
- Vieira, A., J. Vieira, J. Guedes and A. Marques (2009). Experimental degradation characterization of PLA-PCL, PDO, and PGA fibres. International Conference of Composite Materials. Edinburgh, United Kingdom.
- Wei, H. J., C. H. Chen, W. Y. Lee, I. Chiu, S. M. Hwang, W. W. Lin, C. C. Huang, Y. C. Yeh, Y. Chang and H. W. Sung (2008). "Bioengineered cardiac patch constructed from multilayered mesenchymal stem cells for myocardial repair." Biomaterials **29**(26): 3547-3556.
- Wert, K. J., R. J. Davis, J. Sancho-Pelluz, P. M. Nishina and S. H. Tsang (2013). "Gene therapy provides long-term visual function in a pre-clinical model of retinitis pigmentosa." Hum Mol Genet **22**(3): 558-567.
- Xiang, Z., R. Liao, M. S. Kelly and M. Spector (2006). "Collagen-GAG scaffolds grafted onto myocardial infarcts in a rat model: a delivery vehicle for mesenchymal stem cells." Tissue Eng **12**(9): 2467-2478.
- Xiong, Y., J. X. Zhu, Z. Y. Fang, C. G. Zeng, C. Zhang, G. L. Qi, M. H. Li, W. Zhang, D. P. Quan and J. Wan (2012). "Coseeded Schwann cells myelinate neurites from differentiated neural stem cells in neurotrophin-3-loaded PLGA carriers." Int J Nanomedicine **7**: 1977-1989.
- Zajicova, A., K. Pokorna, A. Lencova, M. Krulova, E. Svobodova, S. Kubinova, E. Sykova, M. Pradny, J. Michalek, J. Svobodova, M. Munzarova and V. Holan (2010). "Treatment of ocular surface injuries by limbal and mesenchymal stem cells growing on nanofiber scaffolds." Cell Transplant **19**(10): 1281-1290.
- Zhu, Y., A. Wang, W. Shen, S. Patel, R. Zhang, W. Young and S. Li (2010). "Nanofibrous patches for spinal cord regeneration." Adv Funct Mater **20**(9): 1433-1440.